

## Complex-coordinate method. II. Resonance calculations with correlated target-state wave functions

B. R. Junker

*Office of Naval Research, 800 North Quincy Street, Arlington, Virginia 22030*

(Received 4 August 1978)

We have computed the position and width of the  $1s(2s)^2S$  resonance of  $\text{He}^-$  using five different wave functions for the ground state of He. These wave functions include different amounts of spatial and angular correlation. The difference in the width using a closed-shell target-state function and a three-configuration target function with spatial and angular correlation is only 6.6%. The width using the former function is 12.55 meV, while that for the latter is 11.72 meV. We also performed the calculations without constraining the relative amplitudes of the configurations in the target function to those obtained from a variational calculation of the He ground-state energy. In these calculations we did not encounter the same instability of the complex energy as reported elsewhere in the literature. Finally, improvement in the target-state functions results in a convergence of the scattering-state energies towards the rotated rays. This is to be expected since the description of these states is dominated by the open channel.

### I. INTRODUCTION

The width of an autoionizing or autodetaching Feshbach resonance depends on the coupling of the closed channel with the various possible open channels or continua.<sup>1</sup> Thus all methods which yield resonant positions and widths require a representation of a scatteringlike or  $P$ -space wave function and a representation of a boundlike or  $Q$ -space wave function. The exact partitioning of the total wave function into  $P$  and  $Q$  components is not unique, although the partitioning is generally such that the  $Q$ -space part decays exponentially as any radial coordinate goes to infinity and describes in some manner the closed channel part of the resonant wave function.

The manner in which the two components are used to obtain the resonant positions and widths depends on the method used. In the close-coupling scheme the total wave function is used to obtain a set of coupled differential equations for the scattering function from which a total phase shift is obtained. The resonant parameters are obtained by fitting the cross section to some expression such as a Breit-Wigner expression. Similarly, variational techniques such as the Kohn method yield total phase shifts from which the resonant parameters must be extracted.

The width in the Feshbach formalism is obtained from a Fermi golden rule expression, i.e., it is proportional to the absolute value squared of the matrix element of  $(\mathcal{H}-E)$  with respect to the  $P$ - and  $Q$ -space wave functions. A similar type expression is obtained for the width in the stabilization method<sup>2</sup> assuming the position obtained in a stabilization calculation of  $Q\Psi$  corresponds to the center of the resonance, i.e., where the resonant phase shift

has a value of  $\frac{1}{2}\pi$ .

In another technique known as the complex coordinate method,<sup>3</sup> one employs a non-Hermitian complex Hamiltonian obtained from the normal Hermitian Hamiltonian by transforming all radial coordinates to a radial coordinate multiplied by a phase factor, i.e.,

$$r_i \rightarrow \rho_i e^{i\alpha}. \quad (1)$$

In this method one computes directly a complex energy corresponding to the "resonance". The imaginary part of the energy yields the width via the relation

$$E_I = -\frac{1}{2}\Gamma. \quad (2)$$

In a previous paper,<sup>4</sup> hereafter referred to as I, we suggest that one can better visualize this technique if again one assumes that the wave function consists of a  $P$ - and a  $Q$ -space part. The general properties of these two parts are the same as in the other methods, except that the  $P$ -space part is now square integrable when

$$\alpha > \beta \equiv \frac{1}{2} |\text{Arg}(E_r)|, \quad (3)$$

where  $E_r$  is the complex energy of the pole of the resolvent. For details concerning computations with this method, see I and a related paper<sup>5</sup> which generalizes various aspects of I.

Thus by the nature of the problem, all methods employ a wave function which can be viewed as the sum of two parts—a  $P$ -space part and a  $Q$ -space part. Since the  $Q$ -space part corresponds to closed channels, it is square integrable and presents no problems. On the other hand, the determination of the  $P$ -space part and its coupling to the  $Q$ -space are the problems which the various methods must address. In all of the methods, the  $P$ -space part

is chosen to go asymptotically as the product of the target wave function and the continuum function for the unbound particle. However, exact target functions are known only for one electron target. Generally, single configuration approximations of the target state wave functions are used, although, in principle, one could use, for example, an arbitrarily accurate target-state *CI* wave function in any of the methods. In fact, the only extensive study of the effect of accurate target wave functions is by Bain *et al.*<sup>5</sup> for the  $1s(2s)^2\ ^2S$  resonance of  $\text{He}^-$ . They impose a Gamow or Siegert boundary condition on the wave function to compute the resonant parameters.<sup>7</sup> Their wave function consisted of a *Q*-space type wave function plus a term of the form  $\mathcal{G} \phi_T e^{ikr_0}(1 - e^{-r_0})/r_0$ , where  $\mathcal{G}$  is the antisymmetrizer and  $\phi_T$  is a target function. For target wave functions they used linear combinations of  $1s1s'$ ,  $1s''2s$ , and  $(2p)^2$  configurations. When they restricted the linear coefficients to those obtained from a variational calculation of the  $(1s)^2\ ^1S$  state of He, they obtained results similar to that for just an open-shell target function. On the other hand, when they allowed the coefficients to be determined by the variational calculation of the resonant calculation, the widths obtained were reduced by a factor of about  $\frac{1}{3}$ . Clearly, the limited correlation introduced by the  $1s''2s$  and  $(2p)^2$  configurations should not result in such a drastic reduction. We will return to this point later.

The complex coordinate method is particularly suitable for studying target state correlation. This is because the *P*-space function in this method is square integrable; only a straightforward eigenvalue problem needs to be solved to obtain both the position and width of the resonance, and the only effect of using an accurate target state wave function computationwise is that configurations involving the target state have more Slater determinants to sum over in computing the matrix elements.

In I we presented the results of a calculation of the resonant parameters for the  $1s(2s)^2\ ^2S$  resonance in  $\text{He}^-$ . The target state was represented by an open shell  $1s1s'$  wave function. The widths obtained with various sized wave functions agreed well with transmission experiments but not with differential scattering experiments. In this paper

TABLE I. Linear coefficients.

$\Psi_i \chi_\lambda^i$	$(1s1s')$	$(1s''2s)$	$(2p)^2$
C	0.537 449	-0.013 249	0
D	0.531 835	0	0.017 781 <sup>a</sup>
E	0.538 664	-0.017 780	0.017 881 <sup>a</sup>

<sup>a</sup>This coefficient assumes the function is written as  $\frac{4}{3}^{1/2} (2p_\alpha \alpha 2p_\beta - 2p_0 \alpha 2p_0 \beta + 2p_\alpha \alpha 2p_\beta)$ .

TABLE II. Nonlinear Slater parameters.

$\Psi_i \gamma$	1s	1s'	1s''	2s	2p
A	1.6875				
B	2.1832	1.1886			
C	2.1832	1.1886	2.7023	0.6344	
D	2.1832	1.1886			2.4690
E	2.1832	1.1886	2.7023	0.6344	2.4960

we will give the results of a series of calculations in which a variety of target state wave functions are used. In Sec. II we discuss the various approximate target state functions and their associated variationally determined energies, while in Sec. III we give the computed complex resonant energies resulting from the use of the various target functions. Section IV is devoted to the discussion of the scattering states for the different target functions, and Sec. V summarizes the results. Atomic units are assumed throughout except where explicitly noted otherwise.

## II. TARGET STATE WAVE FUNCTIONS

In previous calculations<sup>8</sup> on the resonant parameters for this resonance closed shell  $(1s)^2$  and open shell  $(1s1s')$ , representations of the target ground state have been employed. The latter allows for a certain amount of spatial correlation. We used this latter function in I.

In addition to these functions, we use three more variational functions which allow for more spatial, as well as angular correlations. This is accomplished by including  $(1s''2s)$  and  $(2p)^2$  configurations. In all, five different wave functions of the form

$$\Psi_i = \sum_\lambda c_\lambda^i \chi_\lambda^i \quad (4)$$

are employed. These are

$$\Psi_A \equiv \mathcal{G}1s(1)1s(2) \quad (5)$$

$$\Psi_B \equiv \mathcal{G}1s(1)1s'(2) \quad (6)$$

$$\Psi_C \equiv \mathcal{G}[c_1 1s(1)1s'(2) + c_2 1s''(1)2s(2)] \quad (7)$$

TABLE III. Variational energies for the five different target functions (experimental energy = 2.903 924).

$\Psi_i$	$E_i$
A	-2.847 16
B	-2.875 02
C	-2.975 98
D	-2.895 17
E	-2.895 69

TABLE IV. Complex energies for various target functions.

$\alpha$ Target	A		B		C		D		E	
	$-E_R$	$-E_I \times 10^3$	$-E_R$	$-E_I \times 10^3$	$-E_R$	$-E_I \times 10^3$	$-E_R$	$-E_I \times 10^3$	$-E_R$	$-E_I \times 10^3$
0.001	2.19075	0.01039	2.19076	0.23000	2.19076	0.21829	2.19082	0.21716	2.19100	0.01791
0.005	2.19076	0.05108	2.19076	0.22290	2.19076	0.22119	2.19082	0.21806	2.19098	0.08470
0.02	2.19076	0.22545	2.19076	0.22285	2.19076	0.22114	2.19082	0.21808	2.19087	0.19765
0.05	2.19072	0.23083	2.19076	0.22282	2.19076	0.22111	2.19082	0.21807	2.19082	0.21543
0.08	2.19072	0.23068	2.19076	0.22282	2.19076	0.22111	2.19082	0.21807	2.19082	0.21545
0.10	2.19072	0.23069	2.19076	0.22282	2.19076	0.22111	2.19082	0.21807	2.19082	0.21545
0.2	2.19072	0.23069	2.19076	0.22282	2.19076	0.22111	2.19082	0.21807	2.19082	0.21545
0.4	2.19072	0.23069	2.19076	0.22282	2.19076	0.22111	2.19082	0.21807	2.19082	0.21545
0.6	2.19072	0.23069	2.19076	0.22282	2.19076	0.22111	2.19082	0.21807	2.19082	0.21545
0.8	2.19072	0.23070	2.19076	0.22287	2.19076	0.22111	2.19082	0.21807	2.19082	0.21545
1.0	2.19072	0.23070	2.19076	0.22287	2.19076	0.22116	2.19082	0.21807	2.19082	0.21545

$$\Psi_D \equiv \mathcal{Q}[c_1 1s(1)1s'(2) + c_2 2p(1)2p(2)] \quad (8)$$

$$\Psi_E \equiv \mathcal{Q}[c_1 1s(1)1s'(2) + c_2 1s''(1)2s(2) + c_3 2p(1)2p(2)] \quad (9)$$

All configurations included the proper spin symmetry. The Slater orbitals are defined as

$$\chi_{nlm}(\vec{r}) = N r^{n-1} e^{-r/r} Y_l^m(\theta, \phi), \quad (10)$$

where  $N$  is the normalization constant.

The linear and nonlinear parameters were obtained from variational calculations and are given in Tables I and II, respectively. Initially, a  $2p2p'$  configuration was used, but after optimization the two nonlinear parameters agreed to within a percent so that they were taken to be equal to reduce the number of integrals. The resulting energies are given in Table III along with the experimental energy.

### III. RESONANCE CALCULATIONS

In I we discuss the partitioning of the total wave function into  $P$ - and  $Q$ -space parts. This partitioning is not unique and does not correspond to a projection via orthogonal projectors. For Feshbach resonances, this partitioning reflects an approximate representation of the open and closed channels, respectively.<sup>9</sup>

In this calculation the  $Q$ -space part consists of the same 31 configurations as in I. The  $P$ -space part consists of four configurations of the form  $\mathcal{Q}(1s1s'ns)$ , where  $ns$  is a Slater orbital which is a function of  $\rho e^{i\alpha}$  and configurations which are antisymmetrized products of target wave functions and "continuum orbitals"<sup>10</sup> of the form

$$\phi_v^* = \exp(\pm i p \rho) \exp(-\delta \rho) [1 - \exp(-\rho)] / \rho. \quad (11)$$

In this calculation the value of  $\rho$  is taken to be 1.19, which is approximately the correct value for  $k$  for this resonance. In I wave functions with 20, 24, and 32  $P$ -space configurations of this latter type were used. By examining the linear coefficients, we were able to select a 16-configuration subset of these and reproduce the results of I. These configurations were those which contained the "continuum orbitals" with the largest values of  $\delta$ , i.e. the  $\delta$  values are 2.5, 2.0, 1.5, 1.0, 0.75, 0.5, 0.25, and 0.1. This simply implies that the most important basis functions are those which describe the nonasymptotic region. This also illustrates why the resonant parameters are not overly sensitive to the value of  $p$ , as we show in I. In these calculations the five different target state functions are used in all 20 of these configurations.

Table IV contains the complex energies obtained with the five different target functions as a function of the rotation angle  $\alpha$ . By comparing the complex

TABLE V. Resonant parameters<sup>a</sup>.

	Position (eV)	Width (meV)
A	19.388	12.55
B	19.387	12.13
C	19.387	12.03
D	19.386	11.87
E	19.386	11.72
F <sup>b</sup>	19.403	11.4
G <sup>b</sup>	19.403	11.1
H <sup>b</sup>	19.403	11.4

<sup>a</sup> From Table III using a ground state energy of  $-79.0016$  eV and a conversion factor of  $27.211652$  eV/a.u.

<sup>b</sup> From Ref. 6, where *F*, *G*, and *H* correspond to target functions *B*, *C*, and *E*, respectively, and a 27-configuration wave function is used. Note that their 48-term wave function yields a position of 19.398 eV and a width of 12 meV.

energies at small  $\alpha$  in Table IV with those of Table V in I, one observes that the effect of including the long-range functions is to yield better complex energies at smaller rotation angles  $\alpha$ . This may arise because the long-range behavior of the unbound electron is described by a function of the form

$$\begin{aligned} \phi &\sim \exp[i|k|\rho e^{i(\alpha-\beta)}] \\ &= \exp[i|k|\rho \cos(\alpha-\beta)] \exp[-|k|\rho \sin(\alpha-\beta)], \end{aligned} \quad (12)$$

where  $\beta$  is defined in (3). As  $\alpha$  approaches  $\beta$  from above, this function extends further and further, becoming unbounded when  $\alpha < \beta$ . Thus inclusion of very long-range functions may be required to adequately describe the resonant wave function near the critical angle  $\beta$ .

Table V contains the resulting resonant parameters. As can be seen, the width decreases as one increases the correlation. On the other hand, the decrease in going from a single configuration closed-shell target function to a three-configuration function with spatial and angular correlation is only 0.83 meV or a reduction of 6.6%. Half of this reduction is obtained by simply opening the  $(1s)^2$  shell.

One must, however, note that since

$$\langle \Psi_P | \Psi_Q \rangle \neq 0 \quad (13)$$

in the manner in which we have decomposed the total wave function, a certain amount of correlation in the *P*-space part is supplied by the *Q*-space part. This is very limited though, since configurations in the *Q* space are such as to basically describe one electron in the vicinity of the nucleus and two elec-

trons removed some distance, whereas the *P*-space part describe at least two electrons near the nucleus.

When Bain *et al.*<sup>6</sup> studied the effect of correlated target wave functions, they performed calculations with target functions *B*, *C*, and *E* in which the  $c_i$ 's were chosen via a variational calculation of the ground-state energy of He or via the resonant calculation of the  $1s(2s)^2S$  resonance in He<sup>-</sup>. They called the first calculation a constrained variation since the relative amplitudes of the configurations were constrained to the values from the atomic calculation on He, and the latter was called an unconstrained variation since the relative amplitudes were allowed to be determined by the variational principle for the resonant calculation. As stated in I, these calculations were performed by imposing a Siegert boundary condition on the variational wave function. This was accomplished by having one configuration in the wave function of the form

$$\psi_B = \mathcal{Q} \phi_T \exp(ikr_0), \quad (14)$$

where

$$E_r = E_R - iE_I = \frac{1}{2} k^2 = \frac{1}{2} |k|^2 e^{-i\theta}. \quad (15)$$

$k$  was determined iteratively by initially assuming some value, computing  $E_r$  variationally, recomputing  $k$  from (15), and recomputing  $E_r$  until  $k$  and  $E_r$  satisfied (15) to some specified accuracy.  $\phi_T$  was only varied in this configuration, although several other configurations were of the form  $\mathcal{Q} \phi_T \phi_{noo}^{STO}$ . In the case of the unconstrained variation with wave function *C*, the value of the width decreased by  $\frac{1}{3}$ , while a similar calculation with function *E* yielded a value for the width which was 25% smaller than in the case of the constrained variational calculations. This type of behavior should not occur if these additional configurations are only describing correlation in the target states. Although it is not obvious why the simple open-shell target function yields what appears to be a very good value for the width, in unpublished calculations using small numbers of *P*-space type configurations, we have found that the width can be a highly oscillatory function until a sufficient number of configurations have been added. A similar type of phenomenon may have occurred in the calculation of Bain *et al.*

To study this further, we also performed unconstrained variational calculations with target functions *C* and *D*. In these calculations, all twenty *P*-space configurations were split into two parts—one containing the  $1s1s'$  and the other containing either  $1s''2s$  or  $(2p)^2$ . Thus the wave functions each contained 71 configurations. The results of these calculations, along with those of Bain *et al.*, are given in Table VI for  $\alpha$  values of 0.08, 0.2,

TABLE VI. Unrestricted variation of coefficients of target configurations.

$\alpha$	C		D	
	$-E_R$	$-E_I \times 10^3$	$-E_R$	$-E_I \times 10^3$
0.08	2.190 83	0.226 93	2.190 85	0.214 45
0.20	2.190 83	0.226 86	2.190 85	0.214 46
0.80	2.190 83	0.226 60	2.190 85	0.214 46
Ref. 6 <sup>a</sup>	2.190 33	0.159	2.190 2 <sup>b</sup>	0.171 <sup>b</sup>

<sup>a</sup> This calculation is independent of  $\alpha$  since it employed only functions of  $\rho e^{i\alpha}$ .

<sup>b</sup> This corresponds to unrestricted variation of target function  $E$ .

and 0.8. From Tables IV and VI, one sees that the width for target function  $C$  changed by only 2.5%, while that for  $D$  changed by less than 0.5%. Due to the negligible change in the width for these unconstrained calculations with functions  $C$  and  $D$ , and the fact that a 91-configuration wave function would have resulted for a similar calculation with target function  $E$ , the latter calculation was not performed. The stability of the energies with regard to the addition of configurations in this calculation tend to indicate that the instabilities observed by Bain *et al.* were probably due to an insufficient description of the  $P$ -space part of the wave function.

## IV. SCATTERING STATES

Many of the eigenvalues correspond to scattering states that should lie on rays which begin at each threshold and make an angle of  $-2\alpha$  with the real axis. In Fig. 1 we have plotted those eigenvalues that can probably be associated with the ray extending from the first threshold for target functions  $A$ ,  $B$ , and  $E$  at a rotation angle of 0.2 radians.<sup>11</sup> As can be seen, the curves described by these eigenvalues approach the ray, which is based on the exact threshold energy as the target trial function is improved. The quality of the target-state function is particularly important for these states, since they correspond to the  $(1s)^2$  channel, and thus most of the configurations in the  $Q$ -space part of the wave function are not important in their description, since these latter configurations correspond to *two* electrons somewhat extended from the nucleus.

Characteristic of these curves, as was observed in I, is the dip. As discussed in I, the energies of these states can be written

$$E = [E_T + \frac{1}{2}|k|^2 \cos(2\alpha)] - i \frac{1}{2}|k|^2 \sin(2\alpha), \quad (16)$$

where  $E_T$  is the threshold energy and  $\frac{1}{2}k^2$  is the energy of the state above threshold. If we identify the value of  $p$  in (11) with  $k$  and recall that the rotation angle is 0.2 radians, we obtain a complex

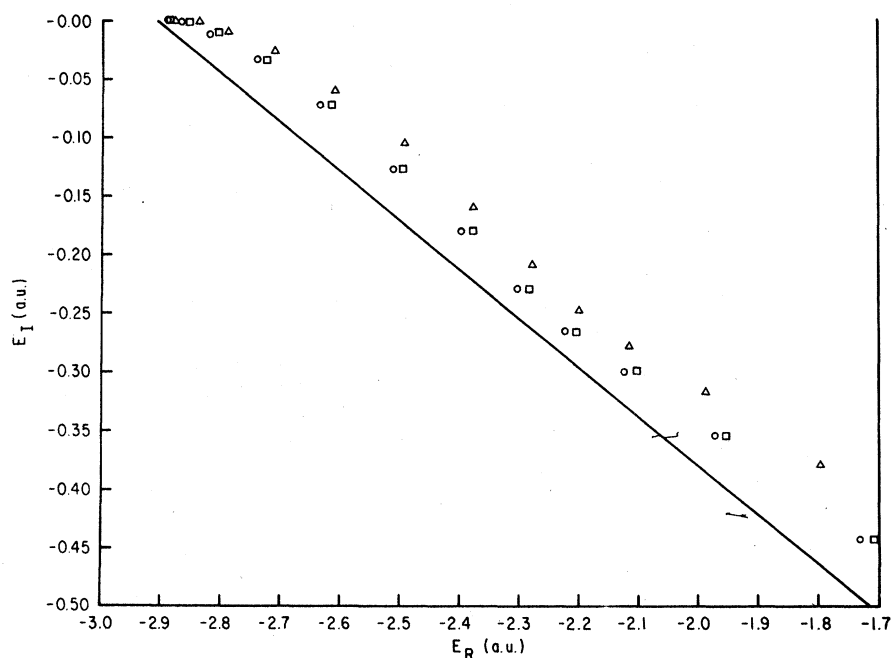


FIG. 1. Complex energies associated with the first threshold for the target functions  $\blacktriangle A$ ,  $\blacksquare B$ , and  $\bullet E$  at a rotation angle of 0.2 radians. The results for target functions  $C$  and  $D$  lie between those for  $B$  and  $E$ .

energy

$$E = (E_T + 0.562) - 0.276i. \quad (17)$$

This is just in the region of the dip. Thus the functions of the form (11) help describe those scattering states, whose energy is in the vicinity of  $\frac{1}{2}p^2$ , best.

In the vicinity of the dip the principal source of discrepancy is now probably correlation in the three-electron system. Further improvement in the target wave function is not likely to be significant since the difference between the experimental energy of the ground state of helium and the variational energy for function  $E$  is only 0.008 a.u. The sources of discrepancy on both sides of the dip are the correlation of the three-electron system and the basis for the description of the unbound electron.

#### V. SUMMARY

We have reported calculations of the  $1s(2s)^2S$  He<sup>-</sup> resonance positions and widths for five different target functions with various amounts of angular and spatial correlation. The width decreased by just 0.83 meV when a closed-shell target function was replaced by a three-configuration target function with angular and spatial correlation. The ground-state energy for this latter function differs from the experimental energy of He by only 0.008 a.u.

In addition, the complex energy was stable with regard to allowing the variational resonance calculation to determine the relative amplitudes of the configurations used to describe the target

ground state. This is in contrast to a previous calculation<sup>6</sup> which suggests the previous wave function did not adequately describe the resonant wave function—particularly the open channel or  $P$ -space part.

Finally, the representation of the scattering states was substantially improved since they are predominantly described by the  $P$ -space part. That is, as the quality of the target-state function improved, the eigenvalues associated with the scattering states of the first threshold converged toward the expected ray. To further improve the description of the scattering states, however, one would have to include correlation of the unbound electron with the target electrons, as well as use an expanded representation of the unbound electron. It should be recalled, though, that the exact scattering states are *not* square integrable.

Although the width in this calculation is not overly sensitive to the quality of the approximate ground-state wave function, this may not be the case for resonances associated with higher thresholds or when several thresholds are very close. For these cases the complex coordinate method is very well adapted to incorporating arbitrarily accurate target-state wave functions in the calculation of the resonant parameters.

I would like to thank Dr. R. Drachman and Dr. A. Bhatia of Goddard Space Flight Center, and Professor J. N. Bardsley of the University of Pittsburgh for critically reading this manuscript. I would also like to acknowledge computer time from Goddard Space Flight Center.

<sup>1</sup>U. Fano, Phys. Rev. **124**, 1866 (1961).

<sup>2</sup>H. S. Taylor and A. U. Hazi, Phys. Rev. A **14**, 2071 (1976).

<sup>3</sup>C. Lovelace, *Strong Interaction and High-Energy Physics*, edited by R. C. Moorehouse (Oliver and Royal, London, 1964); E. Balslev and J. M. Combes, Commun. Math. Phys. **22**, 280 (1971); B. Simon, Commun. Math. Phys. **27**, 1 (1972); B. Simon, Ann. Math. **97**, 242 (1973); C. Van Winter, Math. Anal. App. **49**, 88 (1975).

<sup>4</sup>B. R. Junker and C. L. Huang, Phys. Rev. A **18**, 313 (1978).

<sup>5</sup>B. R. Junker, Int. J. of Quant. Chem. Saimbel Conf Ed. (to be published).

<sup>6</sup>R. A. Bain, J. N. Bardsley, B. R. Junker, and C. V. Sukumar, J. Phys. B: Atom. Molec. Phys. **7**, 2189

(1974).

<sup>7</sup>It can be shown that imposing such a boundary condition on the wave function for real  $r$  corresponds to the analytical continuation of the complex coordinate method back to the real coordinate axis. This was suggested in I and will be discussed further in a later paper.

<sup>8</sup>See I for a list of previous calculations.

<sup>9</sup>See Ref. 5 for a discussion of this partitioning with respect to other processes.

<sup>10</sup>See I for a discussion of these functions.

<sup>11</sup>All other eigenvalues lie near the real axis and have a real part which is greater than  $-2.19$  a.u. This is because the  $P$ -space functions for other thresholds are not well described in our calculation.